

Available online at www.sciencedirect.com

jmr&t
Journal of Materials Research and Technology
www.jmrt.com.br



Original Article

Anisotropic damage of titanium plates under uniaxial tension after reverse bending

Nataliia Shkatulyak^{a,*}, Elena Savchuk^a, Valentin Usou^b

^a Physics Department, South Ukrainian National Pedagogical University named after K.D. Ushinsky, Staroportofrankovskaya Str., 26, Odessa 65020, Ukraine

^b Department of Technological and Professional Education, South Ukrainian National Pedagogical University named after K.D. Ushinsky, Staroportofrankovskaya Str., 26, Odessa 65020, Ukraine

ARTICLE INFO

Article history:

Received 13 February 2017

Accepted 13 June 2017

Available online xxx

Keywords:

Reverse bending

Texture

Young's modulus

Anisotropy

Damage

Titanium sheets

ABSTRACT

Influence of low-cycle reverse bending and the crystallographic texture on damage anisotropy of commercial titanium sheets during the subsequent uniaxial tensile tests was studied. The fourth-rank order damage tensor D was used at the analysis of damage anisotropy of titanium sheets. Only the sole component $D = 1 - \sqrt{E/E_0}$ of this tensor is not equal to zero for uniaxial tension (E_0 and E is the elastic modulus of intact material and current modulus determined from the uniaxial tensile tests, respectively). Damage caused by stresses of proof strength and ultimate strength is estimated. The damage increases with increasing of number of reverse bending cycles. The correlations of damage and mechanical properties anisotropy with the crystallographic texture are found.

© 2017 Brazilian Metallurgical, Materials and Mining Association. Published by Elsevier Editora Ltda. This is an open access article under the CC BY-NC-ND license (<http://creativecommons.org/licenses/by-nc-nd/4.0/>).

1. Introduction

Mechanical or thermal impact is applied in modern technologies for production of metal sheet materials. Internal stress and varied structural defects occur in the metal during production processes. Internal stresses and defects hamper formation of the desired geometric shape of sheet metal, and they can damage the product [1]. Therefore, the straightening by means of machine roller straightening is applied before using of roll metal. Deformation of metal by reverse

bending (RB) occurs in straightening process. Internal stresses are reduced, planar characteristics are improved, and the subsequent processing of metal is facilitated after straightening. All this has a positive effect on the quality of the finished production. Noticeable changes of structure, texture as well as of mechanical characteristics during the reverse bending previously were found, despite the relatively small deformation by the tension and compression of opposite sides of the sheet [2]. Damage in the form of micro-pores, micro-cracks and of their associations may arise at this [3]. Effects of reverse bending and texture on the anisotropy of damage accumulation

* Corresponding author.

E-mail: shkatulyak@mail.ru (N. Shkatulyak).
<http://dx.doi.org/10.1016/j.jmrt.2017.06.007>

2238-7854/© 2017 Brazilian Metallurgical, Materials and Mining Association. Published by Elsevier Editora Ltda. This is an open access article under the CC BY-NC-ND license (<http://creativecommons.org/licenses/by-nc-nd/4.0/>).

in steel sheets during the uniaxial tension were studied earlier in [4,5]. In these studies, the anisotropy of the damage and mechanical characteristics, as well as significant correlation with the characteristics of texture was found [4,5]. The anisotropy of damage coefficient α -titanium textured sheets after cold rolled with 20% and 40% reduction was studied on results of measurements of the dynamic and static Young's modulus in [6]. It is argued that the best agreement with the experimental anisotropy gives an idea of damage tensor as tensor of 6th rank, while the tensor of the 2nd rank gives only satisfactory agreement. In [7] investigated damage coefficient of titanium alloy Ti-6Al-4V after annealing. As the measure of damage, the degradation of Young's modulus material has been used as one of the more effective techniques [8]. Series of loading-unloading experimental tests were carried out and elaborated by means of numerical models in order to build the experimental damage evolution curve. Authors [7] have received very low value of damage in the order of 0.1 for titanium alloy. Similar results were obtained by authors [8] for copper and steel. They believe that despite the popularity of the Young's modulus degradation method for evaluating damage accumulation in structural materials, there is a certain theoretical and practical difficulties in the proper application of this method to receiving of encouraging results. Therefore, according to the authors [7] there is the need of additional studies to clarify the use of aforementioned techniques. Damage coefficients in papers [6-8] were calculated according to the formula [9]

$$D = 1 - \frac{E}{E_0}, \quad (1)$$

where E_0 and E is, respectively, the elastic modulus of intact material and current modulus that determined from the uniaxial tensile tests. Formula (1) was obtained under the assumption of an isotropic accumulation of damages in the metal [9]. At the same time, in order to calculate the damage coefficient D in [10-13], an alternative variant was proposed, which seems to be more justified for the anisotropic accumulation of damages in the metal. The damage is represented by a fourth-rank tensor. Earlier it was shown that under the conditions of uniaxial tension only the single component D of this tensor is nonzero [10,13]:

$$D = 1 - \sqrt{E/E_0}. \quad (2)$$

The notation in (2) is the same as in (1).

This work is aimed to find laws of influence of low-cycle reverse bending (RB) and crystallographic texture on the anisotropy of mechanical properties and damage coefficient of commercial titanium sheets by means of uniaxial tensile tests of samples carved in differ directions of titanium sheets after various numbers of reverse bending cycles.

Effect of reverse bending and texture on the damage coefficient anisotropy during the subsequent uniaxial tensile tests in sheets of titanium and its alloys earlier have not been studied.

2. Experimental material and procedures

Sheets of α -titanium alloy of grade 1 (3.7025) (0.15% Fe; 0.06% C; 0.05% N; 0.12% O, 0.013% H) in the delivery state after annealing at the temperature of 840 °C were used as material for the study. Initial sheets were cut on the cards of size 100 mm × 100 mm. Then these cards were subjected to the RB in the rolling direction (RD) using specifically manufactured device by roller of 50 mm diameter. The speed of the metal movement during bending was about 150 mm/s. From the initial sheet and sheets after reverse bending on 0.5; 1; 3 and 5 cycles were cut at least three batches for each cycle number for mechanical tests in the RD, the diagonal direction (DD, i.e. at an angle of 45° to the RD) and the transverse direction (TD) as well as samples for researches of the texture.

Testing machine Zwick Z250/SN5A with power sensor at 20 kN was used for mechanical tests at room temperature for samples cut in the RD, DD and TD. Samples for tests had total length and width of the working part, respectively, of 90 and 12.5 mm. The average value by at least three batches of samples in each direction was taken as the mechanical property values.

Surfaces of samples were chemically polished to a depth of 0.1 mm for the removing of the distorted surface layer before the texture study.

X-Ray diffractometer DRON-3M was used for the study of crystallographic texture. Recording of diffractograms of the sample without texture as well as textured samples was carried out in the filtered $K\alpha$ Mo radiation. Then inverse pole figures (IPF) for ND of two surfaces of samples after the above-mentioned number of RB cycles were constructed. We constructed also IPF for directions, in which mechanical properties were investigated: RD, DD and TD. In order to provide a flat surface for recording of diffractograms from surfaces perpendicular to the RD, DD and TD strips of 3 mm wide were cut out in the corresponding directions. These strips then were glued to obtain the composite samples.

Investigation of microstructure was carried out at the end faces of samples orthogonal to the RD and TD by microscope MIM-7 using Web-camera E-TREK DEM 200 to output the image structure on the computer monitor.

The symmetrical damage tensor of fourth order D [10-13] was used at the analysis of damage anisotropy of titanium sheets. Only the sole component of this tensor, which was calculated by Eq. (2) is not equal to zero for uniaxial tension (E_0 and E is the elastic modulus of intact material and current modulus determined from the uniaxial tensile tests, respectively) [10,13].

3. Results and discussion

Fig. 1 shows IPF ND and IPF RD of titanium in the initial state as well as IPF's ND after different number of cycles of the RB. The corresponding microstructure is shown in Fig. 2.

The increased pole density on IPF's ND of the initial sheet (Fig. 1, a) covers a wide area bounded by poles $\langle 10\bar{1}5 \rangle$, $\langle 10\bar{1}2 \rangle$, $\langle 11\bar{2}4 \rangle$. In the same time, the absolute maximum of the pole

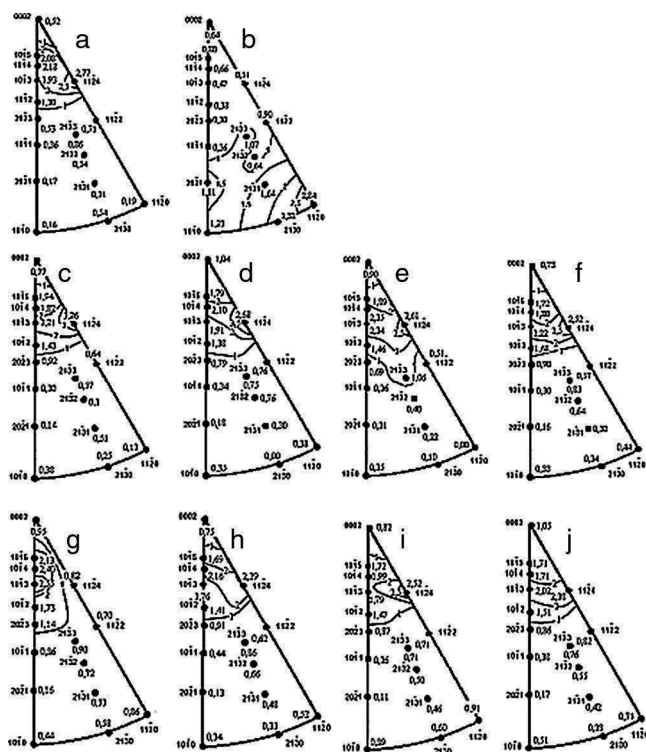


Fig. 1 – Inverse pole figures of titanium sheets: (a, b) corresponds to the ND and RD in the initial state; (c–j) corresponds to the ND after reverse bending during 0.5 (c, d), 1 (e, f), 3 (g, h), and 5 (i, j) cycles; (c, f, g, j) corresponds to the side of sheets subjected to the distension at the first stage of deformation; (d, e, h, i) corresponds to the side of sheets subjected to the compression at the first stage of deformation.

density 2.77 is located in the pole of $\langle 11\bar{2}4 \rangle$, and the local maximum of 2.18 corresponds to a pole of $\langle 10\bar{1}4 \rangle$.

Therefore, the basal plane $\{0001\}$ is inclined from the ND on angles $\pm 30^\circ$ along the side of $\langle 0001 \rangle - \langle 10\bar{1}0 \rangle$ of the stereographic triangle as well as on $\pm 45^\circ$ along the side of $\langle 0001 \rangle - \langle 11\bar{2}0 \rangle$. At the same time on the IPF RD the region of increased pole density is limited by poles $\langle 20\bar{2}1 \rangle$, $\langle 11\bar{2}0 \rangle$, $\langle 21\bar{3}0 \rangle$, $\langle 10\bar{1}0 \rangle$ with an absolute maximum of 2.84 in the pole $\langle 11\bar{2}0 \rangle$ and a local maximum of 1.81 in the pole $\langle 20\bar{2}1 \rangle$.

The area near the pole of $\langle 20\bar{2}1 \rangle$ corresponds to orientations, which are caused by twinning on crystallographic planes of $\{10\bar{1}1\}$ [14]. Thus, in the initial sheet formed texture, which is a combination of annealing twins (Fig. 2) with recrystallization texture of double basal type deflected to the TD. This texture can be described as $\{11\bar{2}4\} \langle 11\bar{2}0 \rangle$ with the scattering to $\{10\bar{1}4\} \langle 10\bar{1}0 \rangle$. Such texture was previously described, in particular, in [7,8]. All the studied titanium sheets have the texture of a double deflected in TD basal type. However, the deflection angle and the pole density are changed depending on the number of RB cycles (Fig. 1). Such changes in the texture at different stages of the RB indicate processes of deformation by slipping and twinning. According to [14], the forming of the said texture is provided as a result of the

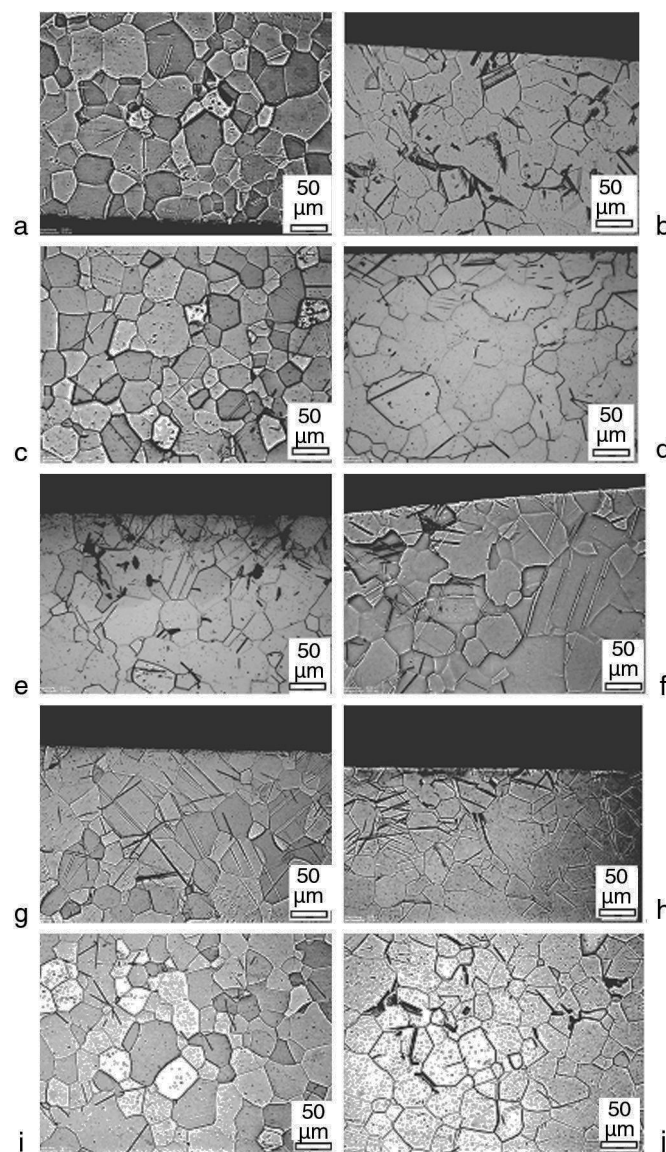


Fig. 2 – The microstructure of titanium sheets in sections perpendicular to the RD (a, c, e, g, i) and TD (b, d, f, h, j); (a, b) corresponds to the initial state; (c–j) corresponds to the state after reverse bending on 0.5; 1; 3; 5 cycles, respectively.

dynamic equilibrium of changes of crystals orientations at pyramidal and prismatic slipping in the direction of $\langle 11\bar{2}0 \rangle$, on the one hand, and twinning, on the other hand. After deformation by 0.5 cycle the RB (Fig. 1c and d) texture is similar to the texture of the initial sheet (Fig. 1a). However, the maximal value of the pole density on the IPF ND became greater on the sheet side, which subjected to the stretching at a bend (Fig. 1c). Increasing of the density basal pole to 1.04 (Fig. 1d) takes place. This indicates an increase in the role of the basal slip in connection with the suppression of twinning [14].

Such trend is confirmed by decrease in the number of twins on the respective micrographs (Fig. 2c and d). Distribution of crystalline orientations after 1 cycle of RB (Fig. 1e and f) became similar to texture of titanium sheet after deformation

0.5 cycles of RB. However, pole density of the base component had decreased and became less than 1 in contrast to the stage of 0.5 cycle of RB. It testifies that the role of the basal slip had diminished and twinning role increased. Increase of twins' number on respective micrographs (Fig. 2e and f) takes place.

At the same time, the form of twins on micrographs obtained from end faces perpendicular to the RD and TD are different. In the section perpendicular to the RD, twins are thinner compared to twins in the section perpendicular to the TD. In the section perpendicular to the TD twins are broader and sharp at the ends, which are typical for the twins $\{10\bar{1}2\}$ [15]. It can be assumed that in the section perpendicular to the TD after 1 cycle of the RB prevail twins broad and sharp on ends, while in the section perpendicular to the RD are observed thin twins as well as paired twins [8]. Texture can be described mainly as $\{10\bar{1}3\} \langle 11\bar{2}0 \rangle$ with the scattering up to the orientation of $\{11\bar{2}4\} \langle 11\bar{2}0 \rangle$ after deformation by 3 cycles of the RB. At this, the number of twins increased on respective micrographs (Fig. 2g and h). In the section perpendicular to the RD observed primarily twins broad and sharp on ends. At the same time, there are also thin twins and paired twins. In the section perpendicular to the TD it is observed a greater number of thin twins, although there are also twins broad and sharp on ends as well as paired twins. Thus, the texture that formed on the deformation stage of 3 cycles by RB may be the result of the dynamic equilibrium of the twinning and pyramidal and prismatic slip [15].

Mechanism of basal slip is activated and role of twinning is weakened in the result of 5 cycles of reverse bending, since the tendency of the increasing of the basal texture is observed (Fig. 1i and j). An indication of this is, on the one hand, increasing the pole density of the basal texture components to a value of 1.05 (Fig. 1j). On the other hand, had decreased the amount of observed twins on corresponding micrographs (Fig. 2i and j).

In the framework of continuum mechanics, the change of the material structure can be described by means of 5 ranges of the damage D : no damage (starts from the limit of elasticity), minor, repairable, unrepeatable and progressive destruction (begins from ultimate strength). Such damage stages can be applied also to the analysis of mechanical stress-strain tests [16].

We evaluated the damage from tests data on uniaxial tensile at stresses that are corresponded to proof strength ($D_{0.2}$) and ultimate strength (D_m). Results of mechanical tests and the damage after different number of RB cycles are shown in Fig. 3. The damage coefficients $D_{0.2}$ and D_m were calculated by the relation (2). We were interested in changes of damage coefficients at uniaxial tensile tests of samples cutout in various directions of titanium sheets, previously deformed by a different number of RB cycles. After deformation by an RB by 0.5; 1; 3 and 5 cycles, the titanium sheets had received the original planar shape. The thickness of sheets did not change at this time. Then we cut out the specimens from the deformed in this way sheets in the above-mentioned directions and carried out uniaxial tension tests. When calculating the damage coefficient as the initial value of the elastic modulus E_0 , we adopted a tabular value for commercial titanium, namely $E_0 = 110$ GPa [17].

Table 1 – Young's modulus of titanium samples under stresses of the conditional yield strength and ultimate tensile strength after various RB cycles numbers.

Cycles	$E(\sigma_{0.2})$, GPa			$E(\sigma_m)$, GPa		
	RD	DD	TD	RD	DD	TD
0	46.3	–	52.3	3.5	–	3.63
0.5	41.0	46.6	57.2	1.0	4.0	4.4
1	45.2	44.7	45.2	5.3	4.7	1.1
3	43.3	48.5	51.0	1.1	5.3	5.7
5	31.4	39.7	29.3	8.9	3.1	0.9

Values of Young's modulus of titanium samples in different directions of the sheets found by means of uniaxial tensile tests under stresses of the conditional yield strength and ultimate tensile strength after various RB cycles numbers are presented in Table 1. In general, the Young's modulus are decreased with increasing number of RB cycles. Periodic changes of the Young's modulus take place. Young's modulus decreases in RD, increases in TD after 0.5 RB cycles. After 1 RB cycles, the Young's modulus has the same value in all three of above directions. After 3 RB cycles, a regularity is observed, marked for 0.5 RB cycles, but for smaller values of the Young's modulus. Young's modulus decrease again after 5 RB cycles. In this case, the values of Young's modulus in RD and TD become smaller than in DD. Analogous periodic variations of Young's modulus but at smaller amplitude also occur at stresses of ultimate tensile strength.

Above we mentioned about periodic changes in the texture character for different number of RB cycles. It is likely that changes in the texture character, Young's modulus and damage coefficients are interrelated.

Stress states of titanium sheets during the RB are changed in sign and thickness, as well as changed their texture, some damages are accumulated (for example, micro pores, and possibly micro cracks). Then, during the uniaxial tension tests the stress state inherent to each specimen cut out from the sheet in different directions is uniformly, at least until the onset of the neck. At this, damages continue to accumulate, due to the action of various sliding and twinning systems that are linked to the texture formed earlier during the RB. Thus, by studying the patterns of the change in the damage coefficient in the initial samples, and also after different number of RB cycles, it is possible to estimate the total accumulation of damages as a function of the number of RB cycles and texture at tests on the uniaxial tension.

Anisotropy of mechanical properties and damage D are observed (Fig. 3). Coefficient k of anisotropy was calculated by the following formula

$$k = \left[\frac{(F_{\max} - F_{\min})}{F_{\min}} \right] \times 100\%. \quad (3)$$

Here F is the corresponding property.

Titanium sheets have minimum values of the coefficient of anisotropy of mechanical properties (k is no more than 1%) in the initial state. Anisotropy coefficient of σ_m reaches the maximum value of 4.7% after 1 cycle of RB, and then decreases slightly, and assumes the value of 4.1% after 5 cycles. Anisotropy coefficients of $\sigma_{0.2}$ and ε reach a maximum after

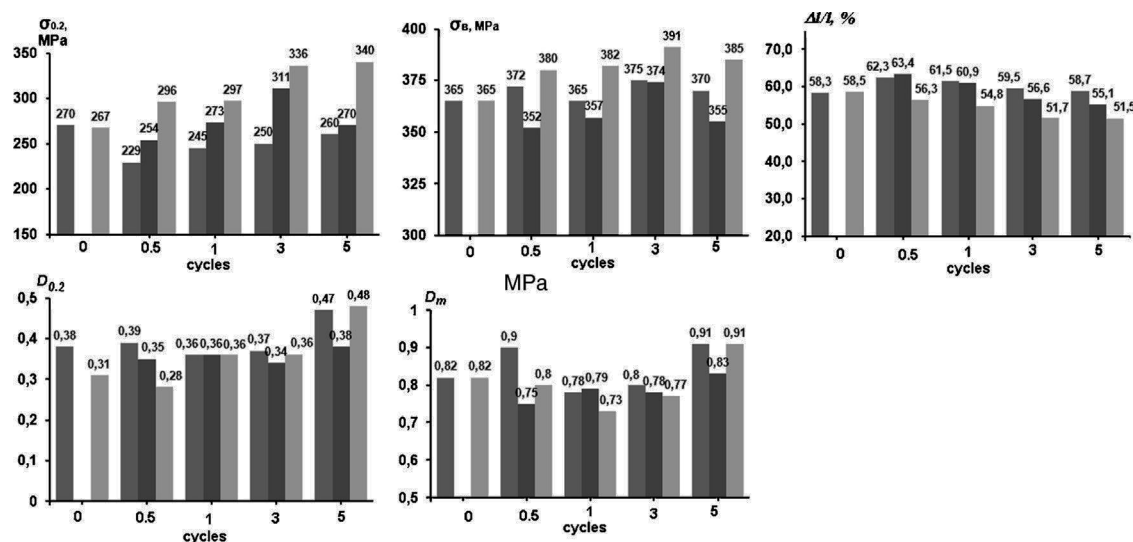


Fig. 3 – Dependence of tensile strength σ_m , proof strength $\sigma_{0.2}$, relative extension $\varepsilon = \Delta l/l$, %, and damage $D_{0.2}$ and D_m from the number of RB cycles.

3 cycles of RB (34% and 15%, respectively). Their values are reduced after 5 cycles of the RB to 31% and 14%, respectively, for $\sigma_{0.2}$ and ε .

Anisotropy coefficient of $D_{0.2}$ is minimal ($k=0$) after 1 cycle of the RB, while anisotropy coefficient of D_m becomes minimal ($k=3.9\%$) after 3 cycles of the RB.

Strong correlations between the damage values $D_{0.2}^{av}$ as well as D_m^{av} averaged by the direction of sheets and number of the RB cycles n were found. Corresponding regression equations and the coefficients of the approximation reliability have the form

$$D_{0.2} = 0.006n^2 - 0.013n + 0.3524; \quad R^2 = 0.95; \quad (4)$$

$$D_m = 0.013n^2 - 0.056n + 0.826; \quad R^2 = 0.92. \quad (5)$$

The proof strength $\sigma_{0.2}$ of the sample after bend on the 0.5 cycle of the RB falls in RD and increases with the increasing the cycles number but the initial value (for the original sheet) is not reached. Value of $\sigma_{0.2}$ in the TD is growing at the deformation up to 3 cycles of the RB, and then stabilizes around a certain value.

Ultimate strength σ_m after deformation by the RB changes less than $\sigma_{0.2}$, and he fluctuated near some average. This characteristic has a minimum value in the DD (i.e. RD + 45°). Mean values of these characteristics increase with increasing number of RB cycles, reach a maximum after 3 cycles of the RB, and decreased with further increase in the number of cycles. Elongation shows the opposite trend: after 3 cycles of the RB is observed a local minimum.

Let us analyze the observed anisotropy of mechanical properties and its variation in the connection with the crystallographic texture after appropriate cycles of the RB. Crystallographic directions of $\langle 11\bar{2}0 \rangle$, $\langle 10\bar{1}0 \rangle$, $\langle 21\bar{2}0 \rangle$ on IPFs of are mostly the same with appropriate directions of sheets of RD, DD and TD. By themselves variations of these orientations do not contribute to the mechanical properties anisotropy,

which is determined by the relative proportions of the orientations close to the $[0001]$ direction, for which twin systems or $(c+a)$ slip must be activated, since Schmid's factors for prismatic slip are close to zero for them. Above it was shown that the texture of investigated titanium sheets can be described by arrangement parallel to the rolling plane of crystallographic planes $\{10\bar{1}3\}$, $\{10\bar{1}4\}$, $\{10\bar{1}5\}$ with scattering up to $\{1124\}$ including $\{0001\}$, with different pole density, depending of RB cycles number. In this case crystallographic directions $\langle 11\bar{2}0 \rangle$, $\langle 10\bar{1}0 \rangle$, $\langle 21\bar{2}0 \rangle$ (that lie in the above-mentioned crystallographic planes) coincide in the main with the RD, DD (i.e., RD + 45°) and TD (Fig. 1). This texture is consistent with earlier results of the study of titanium texture. With this texture, the hexagonal axis c of hexagonal prism is inclined from ND to 30–40° to the TD [18]. Earlier it was shown [19] that, depending on the location of the tension axis in the RD or TD, the active deformation mechanism may differ. If the tension axis is located in the RD, the deformation can be effected by the action of an easier prismatic sliding mode. When the stretching axis coincides with TD, the deformation mode will be more difficult by $(c+a)$, twin system or basal slip, for which the critical resolved slip stress is four times greater than for prismatic sliding at room temperature. In the same directions samples were stretched during mechanical tests. In this context, let us comparable the average pole densities of main orientations determined from the inverse pole figures for selected destinations in the plane of sheets, with the values of the mechanical characteristics of the respective directions (Fig. 3). Appropriate pole densities and their mean values are presented in Table 2.

The analysis showed that with increasing of cycle's number of the RB exist significant nonlinear (quadratic) correlations of values σ_m , $\sigma_{0.2}$, ε , $D_{0.2}$ and D_m with corresponding magnitudes of P_{av} in RD, DD and TD. We have obtained the following regression equations, which together with corresponding coefficients of the approximation reliability are shown in Table 3.

Table 2 – Pole densities $P_{\langle hkl \rangle}$ in ND, DD, and TD as well as their mean values P_{av} for titanium sheets that deformed by reverse bending with different numbers of cycles.

Cycles	RD			DD			TD		
	$P_{\langle 11\bar{2}0 \rangle}$	$P_{\langle 20\bar{1}1 \rangle}$	P_{av}	$P_{\langle 11\bar{2}0 \rangle}$	$P_{\langle 20\bar{1}1 \rangle}$	P_{av}	$P_{\langle 10\bar{1}0 \rangle}$	$P_{\langle 20\bar{1}1 \rangle}$	P_{av}
0	2.84	1.81	2.33	2.69	1.77	2.23	2.78	2.01	2.40
0.5	2.44	1.61	2.03	2.53	1.43	1.98	2.82	2.04	2.43
1	2.61	1.79	2.20	2.7	1.89	2.30	3.18	2.19	2.69
3	2.65	1.85	2.25	3.29	2.3	2.80	3.49	2.43	2.96
5	2.78	1.93	2.36	2.81	2.1	2.46	3.54	2.5	3.02

Table 3 – Results of correlation analysis of mechanical properties, damage and textural characteristics in different directions of titanium sheets subjected to the reverse bending.

Direction in the sheet	Regression equation	Coefficient of the approximation reliability R^2
RD	$\sigma_m = -46.1P_{av}^2 + 171.5P_{av} + 218.6$	0.66
	$\sigma_{0.2} = 82.4P_{av}^2 - 248.4P_{av} + 393.9$	0.89
	$\varepsilon = -20.5P_{av}^2 + 77.5P_{av} - 10.3$	0.89
	$D_{0.2} = 2.5P_{av}^2 - 10.8P_{av} + 12.0$	0.72
	$D_m = 4.3P_{av}^2 - 18.8P_{av} + 21.4$	0.89
DD	$\sigma_m = 42.1P_{av}^2 - 175.8P_{av} + 535.7$	0.94
	$\sigma_{0.2} = 64.8P_{av}^2 - 243.3P_{av} + 393.9$	0.95
	$\varepsilon = 13.2P_{av}^2 - 72.5P_{av} + 155.5$	0.78
	$D_{0.2} = -0.16P_{av}^2 + 0.74P_{av} - 0.50$	0.75
	$D_m = -0.28P_{av}^2 + 1.40P_{av} - 0.91$	0.84
TD	$\sigma_m = -65.2P_{av}^2 + 379.4P_{av} - 163.8$	0.73
	$\sigma_{0.2} = 71.5P_{av}^2 - 287.2P_{av} + 557.0$	0.90
	$\varepsilon = 1.9P_{av}^2 - 20.4P_{av} + 95.8$	0.95
	$D_{0.2} = 0.29P_{av}^2 - 1.33P_{av} + 1.84$	0.75
	$D_m = 1.4P_{av}^2 - 7.5P_{av} + 10.8$	0.81

Thus, the observed anisotropy of mechanical properties and damage as well as their change with increasing cycle's number of the reverse bending carried out largely due to corresponding changes in the texture. At this the greatest changes in the structure, mechanical properties and also in damage occur during the first three–five cycles of the reverse bending.

of the reverse bending. Change in anisotropy of mechanical properties and damage carried out mainly due to crystallographic texture. Significant nonlinear (quadratic) correlations of values σ_m , $\sigma_{0.2}$, ε , $D_{0.2}$ and D_m with corresponding magnitudes of P_{av} in RD, DD and TD were found.

4. Conclusion

- (1) Effect of the reverse bending at room temperature on crystallographic texture, microstructure, and anisotropy of mechanical properties and damage of rolled and annealed titanium sheets was studied.
- (2) Texture in initial (annealed) sheet of commercial titanium is a combination of recrystallization texture double deflected in the transverse direction basal type of $\{11\bar{2}4\} \langle 11\bar{2}0 \rangle$ with the scattering up to orientation $\{10\bar{1}4\} \langle 11\bar{2}0 \rangle$ and annealing twins. Appropriate twins are observed also on photos of the microstructure.
- (3) A certain periodicity is observed in the change of texture $\{11\bar{2}4\} \langle 11\bar{2}0 \rangle$ to the orientation $\{10\bar{1}4\} \langle 11\bar{2}0 \rangle$ and back as well as in formation of the basal components of the texture, amounts and types of deformation twins in the microstructure during the transition from the previous to next cycle of reverse bending.
- (4) The greatest changes in the structure, mechanical properties and damages occur during the first three–five cycles

Conflicts of interest

The authors declare that there is no conflict of interests regarding the publication of this article.

REFERENCES

- [1] Flattening, straightening & leveling; URL: <http://www.arku.com/en/why-roller-leveling/flattening-straightening-leveling.html>.
- [2] Shkatulyak N. Effect of stacking fault energy on the mechanism of texture formation during alternating bending of FCC metals and alloys. Int J Nonferr Metall 2013;2:35–40, <http://dx.doi.org/10.4236/ijnm.2013.22005>. <http://www.scirp.org/journal/ijnm>.
- [3] Gerstein G, Bruchanov AA, Dyachok DV, Nürnberger F. The effect of texture in modeling deformation processes of bcc steel sheets. Mater Lett 2016;164:356–9, <http://dx.doi.org/10.1016/j.matlet.2015.11.007>. www.sciencedirect.com/science/article/pii/S0167577X15308260.

- [4] Shkatulyak N, Savchuk E, Usov V. Anisotropic damage of low-alloy steel plates under uniaxial tension after alternating bending. *Am J Mech Ind Eng* 2016;1:10–4, <http://dx.doi.org/10.11648/j.ajmie.20160102.11>. <http://www.sciencepublishinggroup.com/j/ajmie>.
- [5] Usov VV, Shkatulyak NM, Dragomeretskaya EA, Savchuk ES, Bargan DV, Daskalytsa GV. Effect of alternating bending and texture on anisotropic damage and mechanical properties of stainless steel sheets. *Mech Mater Sci Eng* 2016;6:56–63, <http://dx.doi.org/10.13140/RG.2.2.35491.04640>. <https://issuu.com/mmsejournal/docs/n6>.
- [6] Gokhman AR, Volchok NA. Study of the orientation dependence for damage coefficient of commercial titanium BT1-0 rolled sheets. *FTVD* 2009;19(4):111–7. <http://www.fti.dn.ua/site/en/ftvd-journal/journal-content/ftvd-v19-4/> (in Russian).
- [7] Allahverdzadeh N, Manes A, Giglio M. Application of the elastic modulus degradation technique on the Ti–6Al–4V titanium alloy for CDM models. In: Silva Gomes JF, Vaz Mário AP, editors. *Proceedings ICEM15 15th international conference on experimental mechanics, FEUP – EURASEM – APAET Porto, 22–27 July 2012*. Edições INEGI University of Porto; 2012. ISBN 978-972-8826-26-0, http://paginas.fe.up.pt/clme/icem15/ICEM15_CD/Proceedings.htm.
- [8] Bonora N, Ruggiero A, Gentile D, De Meo S. Practical applicability and limitations of the elastic modulus degradation technique for damage measurements in ductile metals. *Strain* 2010;47:241–54, <http://dx.doi.org/10.1111/j.1475-1305.2009.00678.x>. <http://onlinelibrary.wiley.com/doi/10.1111/j.1475-1305.2009.00678.x/Abstract>.
- [9] Lemaitre J. *A course on damage mechanics*. Berlin: Springer; 1996, <http://dx.doi.org/10.1007/978-3-642-18255-6>. ISBN 978-3-540-60980-3, <https://www.amazon.com/Course-Damage-Mechanics-Jean-Lemaitre/dp/3540609806>.
- [10] Hansen NR, Schreyer HL. A thermodynamically consistent framework for theories of elastoplasticity coupled with damage. *Int J Solids Struct* 1994;31:359–89, [http://dx.doi.org/10.1016/0020-7683\(94\)90112-0](http://dx.doi.org/10.1016/0020-7683(94)90112-0). http://elibrary.matf.bg.ac.rs/bitstream/handle/123456789/3159/Hansen_1.pdf?sequence=1.
- [11] Rashid K, Al-Rub A, Voyiadjis GZ. On the coupling of anisotropic damage and plasticity models for ductile materials. *Int J Solids Struct* 2003;40:2611–43, [http://dx.doi.org/10.1016/S0020-7683\(03\)00109-4](http://dx.doi.org/10.1016/S0020-7683(03)00109-4). <http://abualrub.faculty.masdar.ac.ae/files/Publications/Paper%202.pdf>.
- [12] Bobyr M, Khalimon O, Bondarets O. Phenomenological damage models of anisotropic structural materials. *J Mech Eng* 2013;67:5–13. <http://journal.mmi.kpi.ua/old/article/view/37390>. http://visnyk-mmi.kpi.ua/images/stories/pdf/67/05_Bobyr%20M.PHENOMENOLOGICAL%20DAMAGE%20MODELS.pdf.
- [13] Bobyr NI, Grabovskii AP, Khalimon AP, Timoshenko AV, Maslo AN. Kinetics of scattered fracture in structural metals under elastoplastic deformation. *Strength Mater* 2007;39:237–45. <http://sci-hub.bz/10.1007/s11223-007-0030-4>.
- [14] Wenk H-R, Houtte PV. Texture and anisotropy. *Rep Prog Phys* 2004;67:1367–428, <http://dx.doi.org/10.1088/0034-4885/67/8/R02>. <http://iopscience.iop.org/article/10.1088/0034-4885/67/8/R02/meta>.
- [15] Zwicker U. *Titan und Titanlegierungen*. Berlin-Heidelberg-New York: Springer-Verlag; 1974, <http://dx.doi.org/10.1007/978-3-642-80587-5>. ISBN 978-3-642-80588-2.
- [16] Modirzadeh M, Tesfamariam S, Milani AS. Performance based earthquake evaluation of reinforced concrete buildings using design of experiments. *Expert Syst Appl* 2012;39:2919–26, <http://dx.doi.org/10.1016/j.eswa.2011.08.153>. <http://www.sciencedirect.com/science/article/pii/S095741741101284X>.
- [17] *Titanium and its alloys*; 2000. <http://www.tech.plym.ac.uk/sme/desnotes/titanium.htm>.
- [18] Singh AK, Schwarzer RA. Texture and anisotropy of mechanical properties in titanium and its alloys. *Z Metallkunde* 2000;91(9):702–16. https://www.researchgate.net/publication/279906877_Texture_and_Anisotropy_of_Mechanical_Properties_in_Titanium_and_Its_Alloys.
- [19] Zhu ZS, Liu RY, Yan MG, Cao CX, Gu JL, Chen NP. Texture control and the anisotropy of mechanical properties in titanium sheet. *J Mater Sci* 1997;32(19):5163–7. <http://sci-hub.bz/10.1023/A:1018629819791>.